Flicker Noise in Quasar Light Curves – Statistical Analysis

Shiran Eyal and Oren Gercenshtein

The Hebrew University of Jerusalem, 3rd Year Physics Lab, November 2022

Flicker noise (also known as 1/f noise) peculiarly shows up in a range of very different phenomena across science - from fluctuations in tide and river heights, heartbeat, firings of neurons in the brain, and more. In this study, we first analyze Thermal Noise in an electronic circuit environment, to gain deeper understanding of statistical noise analysis. Consequently, in pursuance of checking the long-lasting assumption that Quasars' time curves are subject to flicker noise, we analyze the statistical properties of the flickering of distant Quasars. We find that although Quasars' light curves have been shown in the past to behave according to a Damped Random Walk model, on our small dataset it appears that the good old flicker-noise model describes the disturbances far better.

I. Introduction

Across various disciplines, from science to art, mankind has always looked up to the skies looking for answers. Galaxies, stars, and other stellar objects never cease to stimulate one's curiosity. In recent years, with rapid advancement in technology, new phenomena are witnessed and studied. Every researcher should have the ability to distinguish irrelevant noise from the signal itself, and from 'good' noise – noise that's part of the measured signal and may be of undenied significance. Therefore, one must understand the different noise models and their origin. In this study we attempt to analyze different types of noise, starting from measuring simple thermal noise, better known as Nyquist noise, on a simple electric circuit. Then, we move on to analyze noise in light curves of Quasars.

II. Theoretical Foundation

Noise

Noise is an unwanted disturbance in a signal. Different types of noise are generated by different devices and different processes. The most common types of noise are Thermal Noise, Shot Noise and Flicker Noise.

Like any stochastic process, noise can be modeled using different statistical tools. Two strong tools for interpreting stochastic processes are the Autocorrelation function and the Power Spectral Density (PSD) function.

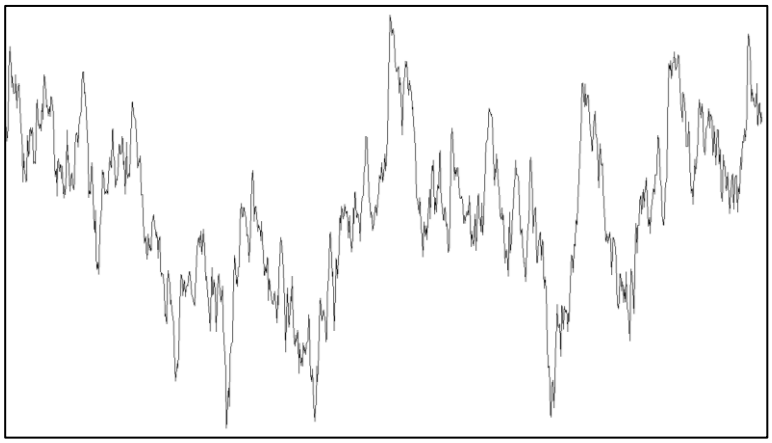

Figure 1.1 – An illustration of white noise.

Autocorrelation function is the correlation of a signal with a delayed copy of itself as a function of the delay. The auto-correlation function of a signal $f(t)$ is defined as:

$$(1.1) \qquad R_{ff}(\tau) \equiv \int_{-\infty}^{\infty} f(t+\tau)\overline{f(t)}$$

The PSD, or power spectrum density of a time-series, describes the distribution of power into frequency components composing that signal.

$$(1.2) \qquad S_{xx}(f) \equiv \lim_{T\to\infty} \frac{1}{T}|\hat{x}(f)|^2$$

The two functions described above are related by Fourier transform (see Wiener–Khinchin theorem), therefore using both functions for signal analysis reveals different aspects of the same signal rather than presenting new/unknown information.

Thermal Noise

Thermal Noise, or Johnson/Nyquist Noise is the electronic noise generated by the thermal agitation of the charge carriers (usually the electrons) inside an electrical conductor at equilibrium, which happens regardless of any applied voltage. Due to its physical origin, thermal noise is white noise – it's random in nature, and its power spectral density is constant (for a considerable part of the spectrum). For an electronic circuit system (the specific system is described in detail in the following chapter), Nyquist reached the theoretical conclusion, later strengthened by Johnson's experiment, that the mean squared voltage created due to thermal noise in a resistor is linearly dependent on its resistance and temperature:

$$V_{rms}^2 = 4k_B TR \int_0^\infty |g(f)|^2 \, df \tag{1.3}$$

Where V_{rms} is the RMS voltage, T stands for the temperature, $g(f)$ for the amplifier's gain-function, R for the resistance and k_B for the infamous Boltzmann constant. The gain function of an amplifier is defined as $\frac{V_{out}}{V_{in}}$, namely the relative increase in voltage due to the amplifier.

Flicker Noise

Flicker noise, also known as 1/f noise, is a signal with a PSD that falls of as $\frac{1}{f^\alpha}$ (for the 1-dimensional case). Therefore, the signal is correlated with itself.

Flicker noise has been discovered in the statistical fluctuations of an extraordinarily diverse number of physical and biological systems (Handel & Chang, 1993). It also describes the statistical structure of many natural images (Field, 1987). Universal theories of pink noise remain a matter of current research interest.

Quasars

A Quasar, also known as a quasi-stellar object, is an extremely luminous active galactic nucleus (AGN), powered by a supermassive black hole, with mass ranging from millions to tens of billions of solar masses, surrounded by a gaseous accretion disc. The energy of Quasars is enormous; the most powerful Quasars have luminosities thousands of times greater than that of a galaxy such as the Milky Way (Wu et al., 2015).

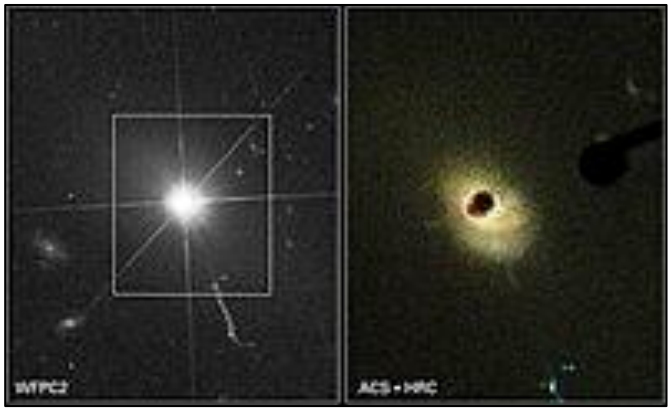

Figure 1.2 - Hubble images of Quasar 3C 273. At right, technology is used to block the Quasar's light, making it easier to detect the surrounding host galaxy.

Quasars are not static objects. Indeed, their light curves vary in magnitude with respect to time. Two models that explain this variation are the starburst and accretion disk instability models (Shakura, 1976). According to the accretion disk instability model, the accretion rate of material onto the Quasar changes over time - the more material accretes onto the Quasar, the less magnitude its light curve obtains. In contrast, the starburst model suggests that the variability is due to supernovae in the surrounding region of the Quasar.

Damped Random Walk

A damped random walk (DRW) is a stochastic process, that behaves as a random walk for short time scales and asymptotically achieves a finite variability amplitude at long time scales.

A DRW is characterized using a PSD as follows:

$$P(f) = \frac{4\sigma\tau}{1+(2\pi\tau f)^2} \tag{1.4}$$

Where σ, τ define certain properties of the signal.

It immediately follows that for larger frequencies, indeed $P(f) \propto \frac{1}{f^2}$.

The Autocorrelation for a DRW is given by:

(1.5) $$ACF(t) = \exp\left(-\frac{t}{\tau}\right)$$

III. Experiment Setup

Resistor noise

Our first experiment consisted of measuring the average root mean square of the voltage $\langle V_{rms} \rangle$ for different resistors over a period of 30 seconds, to confirm the relation predicted in equation (1.3) and confirm the Boltzmann constant from the relation. The following setup was constructed:

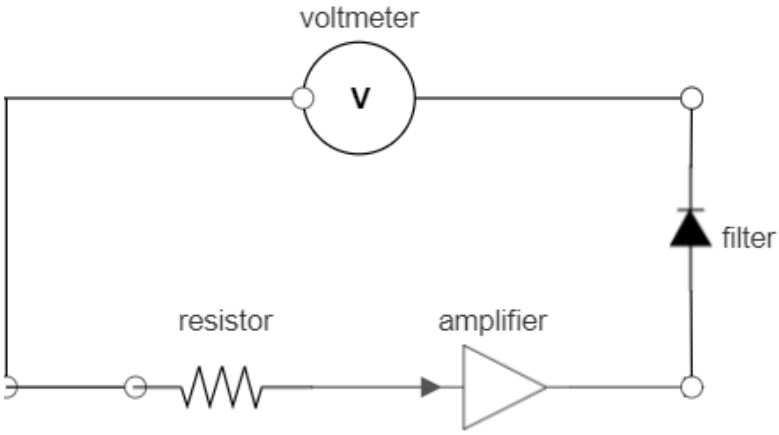

Figure (3.1): Setup Circuit that was used to extract the V_{rms} of each resistor. The circuit consists of a voltmeter that can automatically read V_{rms}, our resistors, an amplifier to amplify the noise of each resistor and a filter.

According to equation (1.3), The extraction of the Boltzmann constant requires us to know beforehand the value of the transfer function of the amplifier that we are working with, to calculate the value of the integral. To do this, we constructed a prerequisite experiment, from which we can extract this value; It was a simple circuit, with current flowing through an amplifier, the one later used for the main experiment. We then measured the voltage before the amplifier (which we call V_{in}) and the voltage after the amplifier (which we call V_{out}). We conducted a series of measurements for $\frac{V_{out}}{V_{in}}$ for different frequencies, which allowed us to calculate $|g(f)|^2$, and numerically calculate the area under the graph, to get a good approximation for the desired integral.

Quasar light curves

Our second experiment consisted of analyzing quasar data from The Sloan Digital Sky Survey (SDSS). We analyzed 9 different quasar light curves that we found and produced autocorrelation and power spectral density plots for all of them, tried different methods of fitting the resulting graphs and compared between the different methods.

IV. Results

Resistor noise

The following graph portrays the plot of the transfer function, e.g., $\left|\frac{V_{in}(f)}{V_{out}(f)}\right|^2$ as a function of f:

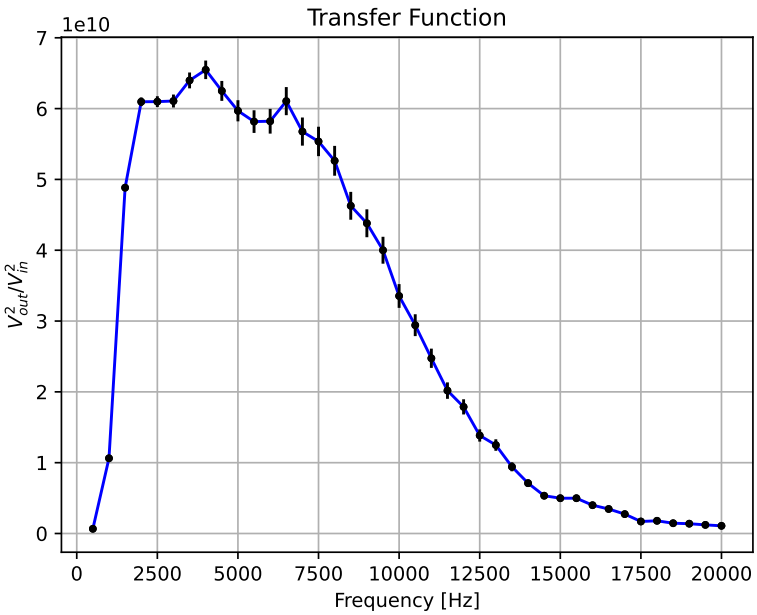

Figure (4.1): The transfer function of the system.

From this graph, the area under the transfer function was calculated, as the average of 2 numerical integration methods - the Trapezoid rule and Simpson's rule. The calculation resulted in a value of:

$$\int_0^\infty |g(f)|^2 df \cong (5.84 \pm 0.03) \cdot 10^{14}$$

In addition to this, we also noticed some noise that the amplifier produces by itself. We took a calibration

measurement of the noise and made a histogram of the resulting data:

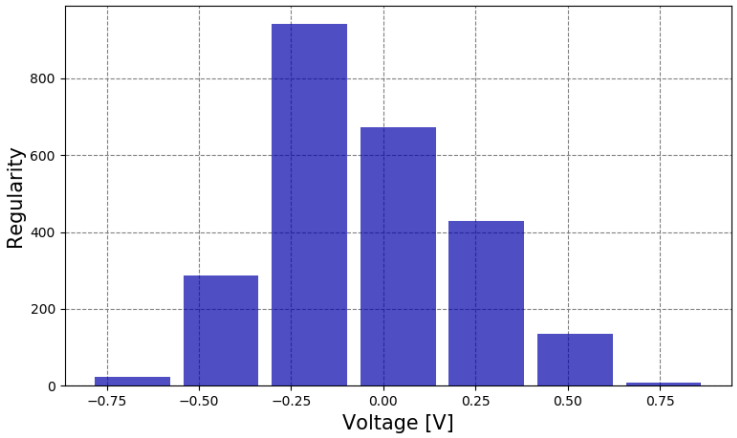

Figure (4.2): Histogram of Amplifier noise during calibration measurement.

Fitting a gaussian curve to this histogram revealed the mean value and standard deviation of this noise to be:

$$\mu = -0.07 \pm 0.04\ [V], \qquad \sigma = 0.27 \pm 0.03\ [\mathrm{V}]$$

This noise was considered when calculating the $\langle V_{rms} \rangle$ on our resistors and their errors. The following graph was constructed using data from all our resistors:

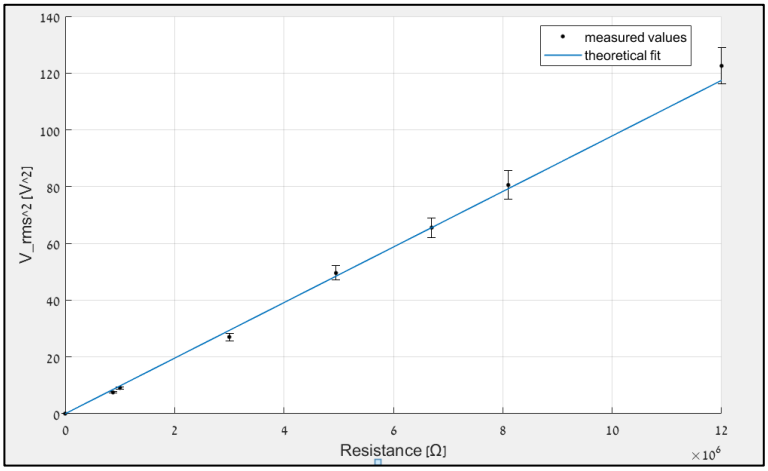

Figure (4.3): Plot of $\langle V_{rms} \rangle^2$ for different resistors, as a function of their resistance. The black dots are the measured points, the blue function is our theoretical fit. Errors were calculated using error advancement of the amplifier noise and the voltmeter noise.

This graph shows a clear linear behavior, almost all of the points error bars pass through the theoretical fit. From this graph we extracted the Boltzmann constant, according to equation (1.1), which yielded a value of:

$$k_B = 1.42 \pm 0.05 \cdot 10^{-23}$$

$$N_\sigma = 0.788$$

This above value appears to be an excellent approximation of the theoretical value of the Boltzmann constant ($1.38 * 10^{-23}$), being less than 1 standard deviation away.

Quasar light curves

We hereby discuss the statistical properties of 2 out of the 9 studied Quasars. The 1st Quasar, which we name F9_B_1m004 (or in short – Quasar 4), and the 2nd Quasar, named F9_B_1m005 (or in short – Quasar 5), are shown in figures (4.4) and (4.5) respectively. The light curves span over ~200 days.

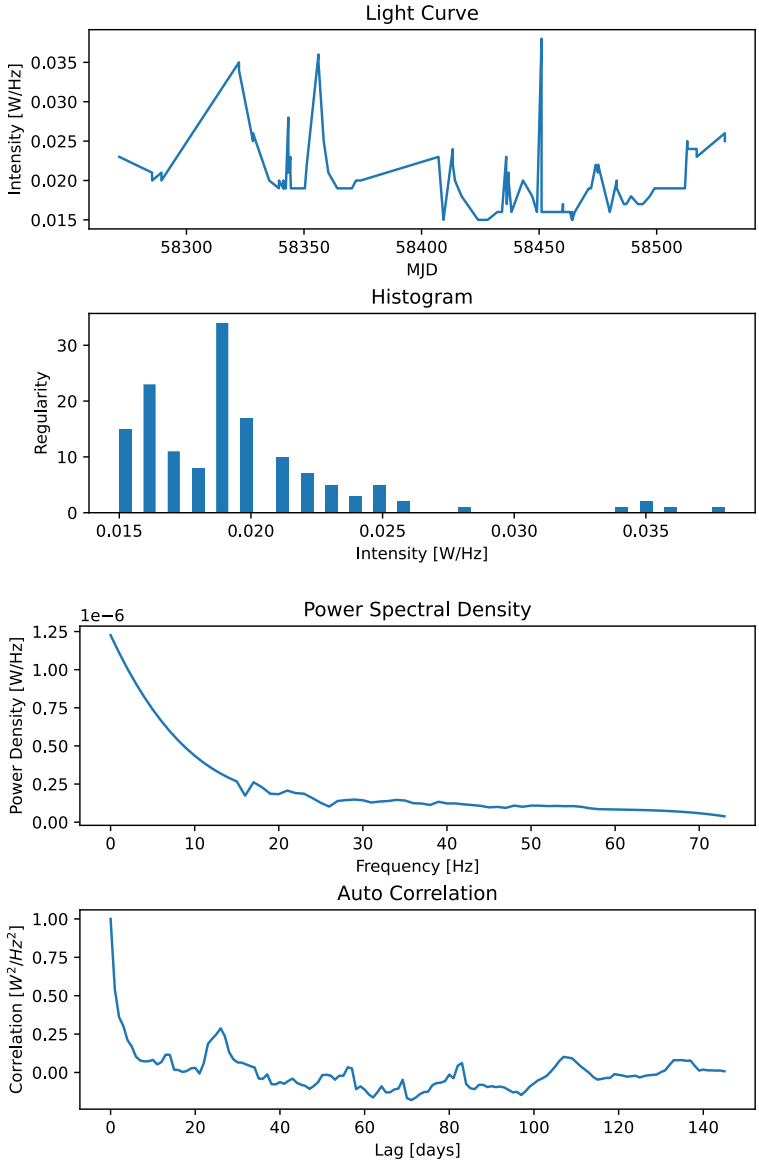

Figure (4.4): Quasar F9_B_1m004 – light curve (top panel), intensities histogram (2nd panel from top), PSD (3rd panel from top) and Autocorrelation (bottom panel).

The histogram of light intensities is plotted with the aim of strengthening the fact that light intensities follow the Boltzmann distribution of $p_i \propto \exp\left(-\frac{E_i}{k_B T}\right)$. From a qualitative point of view, Quasar 4 does exhibit this behavior, but Quasar 5 does not strictly follow it.

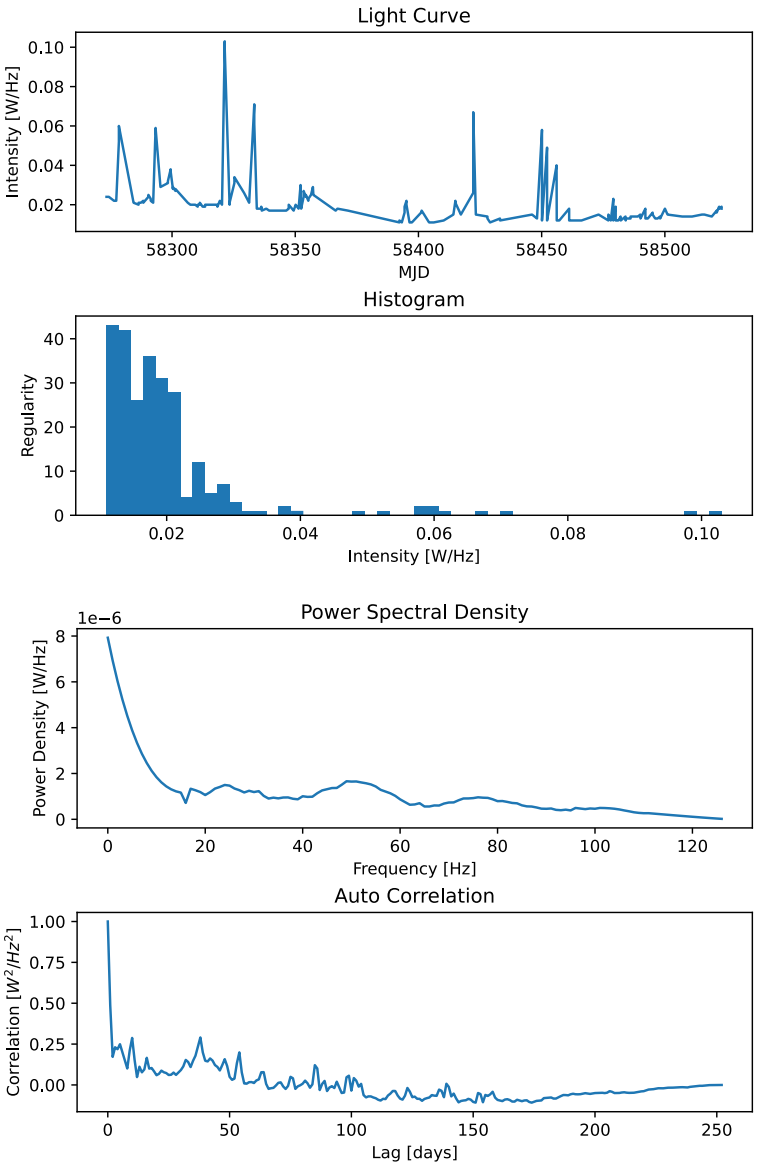

Figure (4.5): Quasar F9_B_1m005 – light curve (top panel), intensities histogram (2nd panel from top), PSD (3rd panel from top) and Autocorrelation (bottom panel).

As for the autocorrelation function, the presented Quasars show impressive resemblance to the accepted theoretical autocorrelation function of pink noise, which qualitatively behaves very similar to a weakly damped harmonic oscillator.

Regarding the PSD, we conducted deeper quantitative analysis, and fitted 2 models to the data, one is the DRW model discussed in Section 2, and the 2nd is flicker noise - $\frac{1}{f^{\alpha}}$ PSD ratio. The fitted models are shown in figure (4.6).

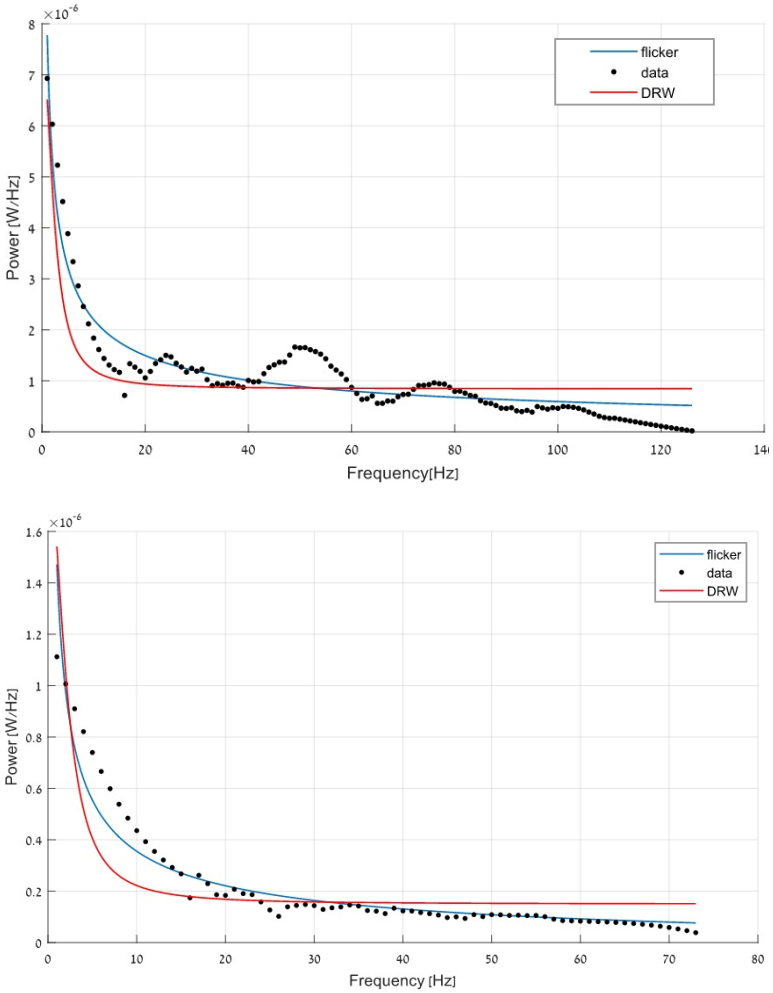

Figure (4.6): Flicker and DRW fit for PSD of Quasar F9_B_1m004 (top panel) and F9_B_1m005 (bottom panel).

The fit parameters are presented in table (4.7).

Quasar	Model	α	R^2
F9_B_1m004	Flicker	0.87 ± 0.05	0.91
	DRW	2	0.72
F9_B_1m005	Flicker	0.85 ± 0.05	0.90
	DRW	2	0.69

Table (4.7): Fit parameters and confidence, for both Quasars. R^2 stands for the confidence in the fit, and α stands for the coefficient the controls the downward curve according to the given model.

As can be clearly seen in table (4.7) and from observing figure (4.6), the model with the best fit confidence is the flicker model, with an α of 0.87.

V. Discussion

In the 1st section of the experiment, we confirmed the Boltzmann constant, using Johnson & Nyquist's formulation for the dependance of RMS-voltage on resistance, temperature, and the system's gain function. Our calculation of the Boltzmann constant was less than a single standard-deviation away from the known value of the constant, which is good enough for our purposes.

We move on to discuss the 2nd part of the study.

The results of this section find that Quasars from our dataset obtain better fits using the $\frac{1}{f^{\alpha}}$ model, rather than using the damped random walk model.

This result is consistent through all 9 Quasars, supporting the fact that it is of real significance.

The autocorrelation function, for all quasars, strongly agrees with the known autocorrelation function of flicker noise, as explicitly shown in the results.

The value obtained for α in the flicker noise model was very consistent, at 0.86 ± 0.05. Although not very far, this value is somewhat different than what we assumed, since past studies have claimed that Quasars exhibit a 'perfect' f^{-1} relation in their PSD.

A few explanations are possible;

First, we know that in astronomical data, most of the time the SNR is very low, and we fear that this is also the situation in our case. Thus, our error and standard deviation may be a lot higher that noted, resulting in a better N_{σ}. Due to our lack of experience with this specific database, it would be of great benefit if research is conducted with aim of validating our findings on a much larger and reliable dataset. Additionally, we think that by choosing to take measurements of quasars on larger timescales, for instance years instead of weeks, we would have been able to make better statistical claims, due to unexpected phenomena that are more likely to occur on smaller timescales than on larger ones.

VI. Appendices

Figure (6.1): The inner workings of the resistor used to lower the input signal into the Amplifier when calculating the transfer function. The resistors were measured and were used to calculate the lowering coefficient.

SPECIFICATIONS: (All at 23°C ± 5°C, 80% R.H.)

DCV:	Ranges	200mV ~ 600V	320mV ~ 1000V
	Resolution	0.1mV	0.1mV
	Accuracy: 0.5% + 2d	.	0.3% + 2d
	Input Resistance: 10MΩ	.	.
	Overload Protection: 1000Vrms	600V rms	.
ACV:	Ranges	200mV ~ 600V	3.2 ~ 750V
	Resolution	0.1mV	1mV
	Accuracy: 1.3% + 5d at 40z ~ 500Hz	.	.
	Input Impedance: 10MΩ//<100pF	.	.
	Overload Protection: 1100VDC or AC peak	600V rms	.
	Conversion Type: Average sensing RMS indicating	.	True RMS
DCA:	Ranges: (20A for 30 seconds)	200μA ~ 10A	320μA ~ 20A
	Resolution	0.1μA	0.1μA
	Accuracy: 1% + 2d basic, 2% + 3d at >2A	.	.
	Input Protection: 1A/500V and 13A/500V fuses, HBC 6000A	.	.
ACA:	Ranges: (20A for 30 seconds)	200μA ~ 10A	320μA ~ 20A
	Resolution	0.1μA	0.1μA
	Accuracy: 1.5% + 3d basic, 2.5% + 5d at >2A all at 40Hz ~ 500Hz	.	.
	Input Protection: Same as DCA	.	.
	Conversion Type: Average sensing RMS indicating	.	True RMS
OHM:	Ranges	200Ω ~ 20MΩ	320Ω ~ 32MΩ
	Resolution	0.1Ω	0.1Ω
	Accuracy: 75% + 4d on 200Ω, 320Ω, 400Ω 75% + 2d on basic ranges 2% + 5d on 20MΩ, 32MΩ, 40MΩ	.	0.5% + 2d basic
	Overload Protection: 500V rms	600V rms	600V rms
CONTINUITY BEEPER:	<50Ω, 2KHz tone buzzer	.	.
DIODE TEST:	Open circuit voltage 3.3V max	.	.
FREQUENCY COUNTER:	Ranges	2KHz ~ 200KHz	.
	Resolution	1Hz	.
	Accuracy: 1% + 3d at 5V rms max	.	.
	Overload Protection: 500V rms	600V rms	.
CAPACITANCE:	Ranges	2nF ~ 200μF	.
	Resolution	1pF	.

Figure (6.2): Data regarding the accuracy of our ohmmeter, as seen in the instruction manual.

■ AC Characteristics

Accuracy Specifications ± (% of reading + % of range) [1]

Function	Range [3]	Frequency	24 Hour [2] 23°C ± 1°C	90 Day 23°C ± 5°C	1 Year 23°C ± 5°C	Temperature Coefficient/°C 0°C – 18°C 28°C – 55°C
True RMS AC Voltage [4]	100.0000 mV	3 Hz – 5 Hz	1.00 + 0.03	1.00 + 0.04	1.00 + 0.04	0.100 + 0.004
		5 Hz – 10 Hz	0.35 + 0.03	0.35 + 0.04	0.35 + 0.04	0.035 + 0.004
		10 Hz – 20 kHz	0.04 + 0.03	0.05 + 0.04	0.06 + 0.04	0.005 + 0.004
		20 kHz – 50 kHz	0.10 + 0.05	0.11 + 0.05	0.12 + 0.05	0.011 + 0.005
		50 kHz – 100 kHz	0.55 + 0.08	0.60 + 0.08	0.60 + 0.08	0.060 + 0.008
		100 kHz – 300 kHz [6]	4.00 + 0.50	4.00 + 0.50	4.00 + 0.50	0.20 + 0.02
	1.000000 V to 750.000 V	3 Hz – 5 Hz	1.00 + 0.02	1.00 + 0.03	1.00 + 0.03	0.100 + 0.003
		5 Hz – 10 Hz	0.35 + 0.02	0.35 + 0.03	0.35 + 0.03	0.035 + 0.003
		10 Hz – 20 kHz	0.04 + 0.02	0.05 + 0.03	0.06 + 0.03	0.005 + 0.003
		20 kHz – 50 kHz	0.10 + 0.04	0.11 + 0.05	0.12 + 0.05	0.011 + 0.005
		50 kHz – 100 kHz [5]	0.55 + 0.08	0.60 + 0.08	0.60 + 0.08	0.060 + 0.008
		100 kHz – 300 kHz [6]	4.00 + 0.50	4.00 + 0.50	4.00 + 0.50	0.20 + 0.02
True RMS AC Current [4]	1.000000 A	3 Hz – 5 Hz	1.00 + 0.04	1.00 + 0.04	1.00 + 0.04	0.100 + 0.006
		5 Hz – 10 Hz	0.30 + 0.04	0.30 + 0.04	0.30 + 0.04	0.035 + 0.006
		10 Hz – 5 kHz	0.10 + 0.04	0.10 + 0.04	0.10 + 0.04	0.015 + 0.006
	3.00000 A	3 Hz – 5 Hz	1.10 + 0.06	1.10 + 0.06	1.10 + 0.06	0.100 + 0.006
		5 Hz – 10 Hz	0.35 + 0.06	0.35 + 0.06	0.35 + 0.06	0.035 + 0.006
		10 Hz – 5 kHz	0.15 + 0.06	0.15 + 0.06	0.15 + 0.06	0.015 + 0.006

Additional Low Frequency Errors (% of reading)

Frequency	Slow	AC Filter Medium	Fast
10 Hz – 20 Hz	0	0.74	—
20 Hz – 40 Hz	0	0.22	—
40 Hz – 100 Hz	0	0.06	0.73
100 Hz – 200 Hz	0	0.01	0.22
200 Hz – 1 kHz	0	0	0.18
> 1 kHz	0	0	0

Additional Crest Factor Errors (non-sinewave) [7]

Crest Factor	Error (% of reading)
1 – 2	0.05%
2 – 3	0.15%
3 – 4	0.30%
4 – 5	0.40%

Figure (6.3): Data regarding the accuracy of our voltmeter, as seen in the instruction manual.

VII. Bibliography

1. J. B. Johnson, THERMAL AGITATION OF ELECTRICITY IN CONDUCTORS, July 1928
2. Ying Zu , C.S. Kochanek, Szymon Koz lowski , and Andrzej Udalski, IS QUASAR OPTICAL VARIABILITY A DAMPED RANDOM WALK?, October 2018.
3. University of Chicago, Sloan Digital Sky Survey (SDSS), 2000.